Influence of Crystal Orientation on Electromechanical Behaviors of Relaxor Ferroelectric P(VDF-TrFE-CTFE) Terpolymer

Qing Liu, Jean-Fabien Capsal, Claude Richard

Abstract—In this current contribution, authors are dedicated to investigate influence of the crystal lamellae orientation on electromechanical behaviors of relaxor ferroelectric Poly (vinylidene fluoride –trifluoroethylene -chlorotrifluoroethylene) (P(VDF-TrFE-CTFE)) films by control of polymer microstructure, aiming to picture the full map of structure-property relationship. In order to define their crystal orientation films, terpolymer films were fabricated by solution-casting, stretching and hot-pressing process. Differential scanning calorimetry, impedance analyzer, and tensile strength techniques were employed to characterize crystallographic parameters, dielectric permittivity, and elastic Young's modulus respectively. In addition, large electrical induced out-of-plane electrostrictive strain was obtained by cantilever beam mode. Consequently, as-casted pristine films exhibited surprisingly high electrostrictive strain 0.1774% due to considerably small value of elastic Young's modulus although relatively low dielectric permittivity. Such reasons contributed to large mechanical elastic energy density. Instead, due to 2 folds increase of elastic Young's modulus and less than 50% augmentation of dielectric constant, fully-crystallized film showed weak electrostrictive behavior and mechanical energy density as well. And subjected to mechanical stretching process, Film C exhibited stronger dielectric constant and out-performed electrostrictive strain over Film B because edge-on crystal lamellae orientation induced by uniaxially mechanical stretch. Hot-press films were compared in term of cooling rate. Rather large electrostrictive strain of 0.2788% for hot-pressed Film D in quenching process was observed although its dielectric permittivity equivalent to that of pristine as-casted Film A, showing highest mechanical elastic energy density value of $359.5 \, J/m^3$. In hot-press cooling process, dielectric permittivity of Film E saw values at 48.8 concomitant with ca.100% increase of Young's modulus. Films with intermediate mechanical energy density were obtained.

Keywords—Crystal orientation, electrostrictive strain, mechanical energy density, permittivity, relaxor ferroelectric.

I. INTRODUCTION

RECENT years saw an emerging interests of electroactive polymers in the actuator [1], transducer [2], artificial muscles [3], [4] and integrated microelectromechanical system (MEMS) applications [5] because of its attractive high electrostrictive strain response and high mechanical energy density. It was reported that electron beam irradiated P (VDF-TrFE) [6] exhibited a larger electrical field induced strain up to about 4% and improved electromechanical coupling factors,

making it as a good candidate for practical sensor and actuator implementation. Most accessible approach to improve the electrostrictive properties of fluorinated polymers is to reduce the crystallite size through introduction of defects. Besides the irradiated PVDF copolymer, random terpolymer Poly(vinylidene fluoride –trifluoroethylene-chlorotrifluoroethylene) [P(VDF-TrFE-CTFE)] or Poly(vinylidene fluoride –trifluoroethylene-chlorofluoroethylene) [P(VDF-TrFE-CFE)] obtained by copolymerized chloride containing ternary monomer –CTFE or -CFE were found as typical ferroelectric polymers with diffusion phase transition. Incorporation of chloride bulk ternary monomer served as a chain defect, could disrupt the all-trans (*Tm*, m>3) ferroelectric nano-domains and lead to a mixture of non-polar para-electric like TG^+TG^- (α-form) crystal lamellae and $T_3G^+T_3G^-$ (γ-form) chain conformation which is apparently non-polar and exhibits relaxor ferroelectric behavior [7]. That is to say, peaks found over isochronal dielectric spectroscopy shifted towards progressively high-field of frequency and temperature. Hence, diffusion phase transition strongly dependent on frequency was common features of fluorinated terpolymers, and thus many have been focusing on its origins. Buckley [8] synthesized novel P(VDF-TrFE-CTFE) terpolymers with compositional variation of CTFE content by means of a novel borane/oxygen initiator, yielding homogeneously ternary distributed terpolymer. And the presence of the bulky CTFE units disrupted the sequence length of the crystal, which lowered both the melting and Curie transitions This could also link to a formation of reduced crystal size and more polar nano-domains. This presented the significantly larger strain than that of terpolymer obtained by using of bulk polymerization as common employed. Bao [9] investigated microstructures and phase transition behaviors of P(VDF-TrFE-CFE) by various processing conditions with respect to annealing temperature, showing that four types of transitions detected including ferroelectric-paraelectric transition and the disrupted all-Trans conformation transformation in spites of dynamic vitreous transition and melting transition. The ferroelectric-like crystal and polar nano-domains were responsible for the dielectric response, which the former was frequency-independent dielectrics related and the latter was relaxor behavior related. Enormous attention was attracted in study of relaxor ferroelectric behavior and its electrostrictive properties. Indeed, fully investigation of relaxor behavior-

Qing Liu, Jean-Fabien Capsal, Claude Richard are with the Université de Lyon, INSA de Lyon, Laboratoire de Génie Electrique et Ferroélectricité (LGEF), EA682, 8 Rue de la Physique, F-69621 Villeurbanne, France (phone: +33 04 72 43 79 53; e-mail: qing.liu@insa-lyon.fr).

electromechanical relations and how Curie transition affects electromechanical behavior were concerned.

In this current study, P(VDF-TrFE-CTFE) terpolymers were employed to investigate influence of process and microstructure factor on dielectric behavior and mechanical properties. Therefore, films were fabricated by casting, mechanical stretching, and hot-press respectively. In addition, their electrostrictive response and mechanical elastic energy density for each film process condition dependent were evaluated in cantilever beam mode.

II. Experimental Section

A. Chemicals and Sample Elaboration

P(VDF-TrFE-CTFE) terpolymers with composition mole ratio of VDF/TrFE/CTFE=61.7/30.4/7.9 was utilized for study by courtesy of Piezotech S.A.S (Arkema Group, France) which was synthesized by a suspension polymerization engineering. Prior to film specimen fabrication, no special pre-treatment were carried out. All the solvents mentioned were provided by Sigma-Aldrich in this present work and used as received without further purification. In order to elucidate the resulting dielectric behaviors and electromechanical properties dependent of terpolymer crystal morphologies in terms of crystallinity and structure, isothermal polymer processing treatments were elaborated to desire the terpolymer crystallinities. Respectively, the transparent dielectric terpolymer solution were prepared by solubilizing the P(VDF-TrFE-CTFE) terpolymer grain in MEK (Meth Ethyl Ketone) solvent in a concentration of 14 wt%. Film A (denominated SCNON Film A) were prepared by solution casting from a 14% terpolymer MEK homogeneous solution with Elcometer blade film applicator, without post annealing processing in thickness of ca. 85 μm. Isothermally annealing specimen were prepared by annealing the Film A in a 120°C oven for 12h designated as Film B (SCAN120C12H Film B), where the temperature got involved within the melting region. Film C (Stretched Film B) was obtained by uniaxially stretched the Film B at 90°C and cooled in an ambient atmosphere. Film D with average thickness approximately 88.6 μm was prepared by hot-pressing as P(VDF-TrFE-CTFE) terpolymers powder by a Carver hydraulic presses (Carver, USA) in a 40 bar pressure at 160°C of both bench top and floor standing for 5 min and then quenching into the ice water (around 0°C). Film E designated as HP-Cooling Film E in thickness of 85 μm was hot-pressed terpolymer grain and followed by cooling down to the room temperature in an ambient atmosphere in cooling rate of 2°C/min. All the labelled specimens were allowed to equilibrate at ambient atmosphere for 24h.

B. Device Fabrication and Characterization Techniques

As-treated terpolymers thermal behaviors were monitored with DSC 131 Setaram Evo equipped with liquid nitrogen cooling accessory. Prior to thermal record, calibration was running with alumina standard and the empty cell was also running as baseline. Each specimen with normalized simple weight running upon the identical heating and cooling phase was heated in an increment of 10°C/min with probe temperature range from 183K to 473K under nitrogen flow rate of 1.5 bar. Young's modulus was obtained by non-conventional strength tensile mechanical analyzer. The deformation and strain rate of sample was driven by a function generator through the controlled Newport platform and Labview. The tensile force was recorded by an explicit force sensor. 40mm normalized length of films was conducted. Sinusoidal signal (0.1Hz) was subject to the motor and true sinusoidal strain (1% maximum set) resulted the loading-unloading cycles. Dielectric permittivity was carried out by Solartron 1260 (UK) impedance-analyzer equipped with Model 129610A LHe LN2 Cryostat System. As-deposited dielectric terpolymers circular films plates in diameter of 20 mm were metalized by sputtering gold on both surfaces through shadow mask. The metal/polymer/metal parallel plate capacitor was subjected to the impedance-analyzer. Dielectric spectroscopy data acquisition were conducted with electric field frequency in a probe sweeping range from 10^{-1} to 10^6 Hz at a low level of AC 1V electric potential under ambient temperature 25°C. Electrical breakdown strength was acquired with home-made equipment. Circular metal/polymer/metal capacitor samples with 10mm diameter gold sputtered wetted and immersed into silicon oil were clamped between a needle-like copper electrodes. A DC high voltage was applied in a ramp rate of 2 kV/3s until electrical current induced mechanical failure.

Unimorph cantilever beam transverse strain measurements were carried out in a protocol with set-ups described elsewhere [10]. Laser sensor was performed to monitor unimorph tip displacement induced by external field perpendicular to the longitudinal direction of unimorph. Combined polymer mechanical behavior, tip displacement (δ) reads:

$$\delta = \frac{3L^2}{2t} \frac{2\lambda\xi(1+\xi)^2}{\lambda^2\xi^4 + 2\lambda\xi(2+3\xi+2\xi^2)+1} S_{31} \qquad (1)$$

where; L, t is unimorph's length and thickness related to its dimension, λ represents the Young's modulus ratio of active relaxor ferroelectric polymers to the substrate polystyrene (PS) film (100um); ξ symbolizes the thickness ration of PS substrate to the active polymers, respectively, S_{31} is terpolymer out-of-plane transverse train.

III. Results and Discussions

A. Thermal Behavior and Crystallinity Properties

In light of recent reports dedicated to the influence of crystallinity on the glass transition dynamics, semi-crystalline polymer morphologies induced by processing condition had a considerable impact on the polymer dielectric and mechanical properties, affording us to fully unveil and build morphology (microstructure)-properties relationship between dynamic glass transition process and its contributing factors. As-treated dielectric terpolymer P(VDF-TrFE-CTFE) as typical semi-crystalline one had pseudo-hexagonal packed crystal lamellae with amorphous phase sandwiched [11]. Its isomorphic crystal

forms and microstructure could be deduced by varying polymer processes, e.g. solution-cast, hot-press, uniaxially mechanical stretch and electro-spinning [12]-[14] concomitant with orientated crystal lamellae stacks. And further isothermal treatment allowed the less well-ordered crystal lamellae in matrix induced to well-ordered crystal due to rearrangement of entangled polymer chain.

Fig. 1 gives the DSC thermogram traces of as-treated terpolymers films over a broad temperature range scale. Since that films undergone thermal process history were subjected to the slow cooling ramp from the melt state, the interpretation of similarity of results picked up from the second heating ramp could be facile, of which thermal history were thoroughly eliminated. Thereafter, glass transition process was hardly discernible (barely detectable) in the normal heat flow gram traces for each films. Basically, C-C single bond backboned molecular chain segments for nature of P(VDF-TrFE-CTFE) were facile to be activated. Therefore, increment of heat capacity (ΔC_P) for P(VDF-TrFE-CTFE) was noticeably little over the DSC thermal gram traces only by which glass transition dynamics were not accessible. Briefly, two discernible endothermic peaks, of which the small ones were Curie transition related located at lower temperature at around 40 °C and the broad and intense phase regimes were corresponding to melting regions at higher temperature, would be the common features. Nonetheless, their peak position, integral value and full width at high maximal of melting peaks

were processing dependent, as an indicative of variation of microstructure in crystallographic aspect. Thus glass transition temperature and characteristic parameters related to the peaks and transitions were summarized in Table I.
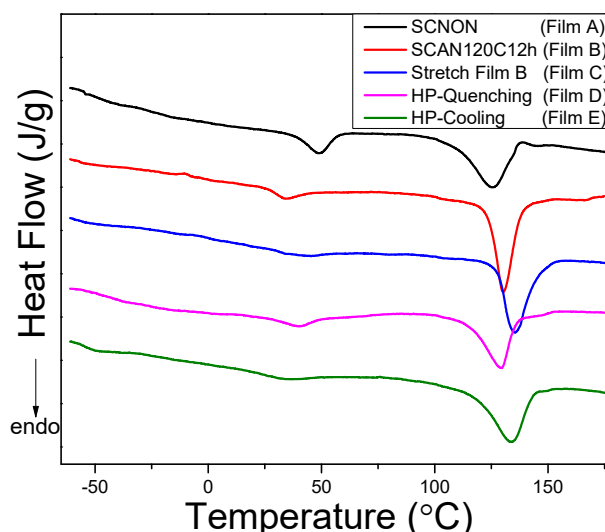

Fig. 1 DSC thermal gram traces of as-casted isothermal-induced, stretched and as-hot pressed terpolymer films

TABLE I
DSC GLASS TRANSITION TEMPERATURE (T_g), CURIE TRANSITION TEMPERATURE (T_{CURIE}), CRYSTALLINITY AND MELTING PEAKS PARAMETERS FOR ALL SEMI-CRYSTALLINE P(VDF-TrFE-CTFE) FILMS STUDIED

Acronym	T_g °C	ΔC_p (mW)	T_{curie} °C	ΔH_{curie} (J/g)	ΔH_m (J/g)	[a]Crystallinity First ramp%	Melting region(°C)	
							T_m	FWHM
SCNON Film A	-27.0	0.148	47.42	4.40	12.95	12.63	125.43	19.73
SCAN120C12H Film B	-23.8	0.070	32.86	2.60	19.02	18.56	130.23	7.988
Stretched Film C	-23.5	0.074	39.55	2.89	17.56	17.13	135.37	16.03
HP-Quenching Film D	-25.6	0.101	40.17	2.70	14.65	14.29	129.45	20.35
HP-Cooling Film E	-20.9	0.168	34.38	2.86	17.16	16.74	133.68	25.42

Note: Crystallinity of each polymer (χ_c) were calculated from the integration of curves by the formula of $\chi_c = \Delta H_f / \Delta H^*_f \times 100\%$, where ΔH_f is enthalpy of fusion of as-treated semi-crystalline polymers; ΔH^*_f is the melting enthalpy of crystalline terpolymers consisting of 100% crystallinity. (ΔH_f, $100\% \, crytal$ =102.5(J/g))[8][15].

Concerning intense DSC phase transition peaks, melting region shape showed the variations between the semi-crystalline as-treated terpolymer films. As solution-casting samples, crystallinity χ_c abruptly increased from 12.63% for pristine film A to 18.56% for the far isothermal crystallized Film B, due to which the melting temperatures saw a significant shift toward higher temperature from 125.38 °C to 130.28 °C. Surprisingly, degree of crystallinity for stretched film was slightly lower than that of original Film B and its melting temperature shifted towards much higher temperature to large degree. Molecular chain randomly entangled in biphase polymer Film A matrix where crystal lamellae orientation was distributed, remaining the memory of chain arrangement used in solution state. When applied induced uniaxial stretch, the crystal lamellae slipped between each

neighboring crystal lamellae and consequently predominant crystal orientation were consistent with stretching force direction. The c-axis of crystal lamellae were in parallel with stretching direction as presented in Fig. 2. Due to the enhancement of homogeneity, associated physico-chemical properties were altered drastically such as thermal traces, dielectric permittivity and mechanical properties of which would be discussed in Section C. On basis of this fact, the elevated melting point could be ascribed to the well-ordered and denser crystal lamellae induced by mechanical stretch. In this point, reduced crystallinity fraction would be rationalized that stretching effects contributed to the decrease of volume fraction of crystal lamellae which used to attach with rigid crystal phase.

The observed similar trend could be seen on the hot-pressed dielectric films of which melting points differed between hot-pressed quenching film D in 129.45℃ and cooling Film E at 133.68℃. These results reflect that crystallinity degree of terpolymers that was induced by thermal treatment changes with film processing procedure alternatively. As shown in Fig. 1, another distinct feature was that Film B and the stretched Film C exhibited extremely sharp endothermic melting peaks. Full widths at high maximum (FWHM) values of film melting region are quite different. FWHM values of as-casted Film B and Film C were much lower than that of hot-pressed Film D and Film E, reflecting that the crystal size distribution were quite homogeneous. These results afforded the homogeneity of thermal behavior inside the crystal phase region. In a second running heat cycle, fusion of enthalpy of each as-prepared films and FWHM temperature values had been uniform after erasing the pre-thermal treatments, showing much larger than that of Film C and Film D. Moreover, heat of fusion increment between Film B and A was much larger than heat of fusion between Film D and Film E, providing a witness that isothermal crystallization has a large contributing factor to the crystallography and microstructure.
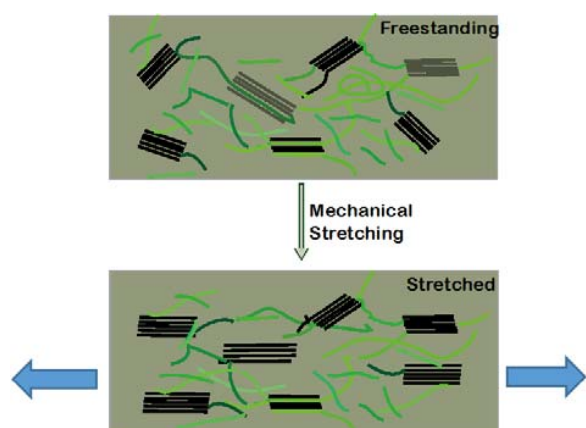

Fig. 2 Schematics of crystal lamellae orientation in stretched Film C

Moreover, less intense endothermic peak near ambient temperature definitely referring to the Curie transition also had large variations, reflecting different dielectric phase transition from ferroelectric to paraelectric behavior. It was clear that α-form (TG^+TG^-) and γ form $(T_3G^+T_3G^-)$ were predominately composed of terpolymer chain conformation, both of which much stable than all Trans(Tm, m>3) β form. Due to the atactic copolyermered ternary CTFE monomer into the P(VDF-TrFE) copolymer chain, the polar β form crystallite was converted into the different metastable γ phase with crystal lattice close to that of the para-electric crystalline α phase. Therefore terpolymers behaved a diffusion phase transition over a large scale of temperature sweeping evidently [16].

As shown in Table I, Film A had a higher curie temperature 47.4 ℃ than that of others which the Curie temperature T_C shifted toward the lower temperature continuously depending on the isothermal crystallization treatment of as-cated films to 32.86℃ for the Film B. It was essential that polymer chain motions occurring in the composed phases induced the elimination of steric hindrance and uniformity of chain arrangement which behaved homogeneity in both crystal phase and amorphous phase. This could lead to a reduction energy barrier of ferroelectric phase transition to the para-electric phase. The more details and forceful evidence could be found as gradual decrease in Curie phase transition enthalpy from 4.4 J/g for Film A to 2.60 J/g for film B, respectively. As for the hot-pressed Film D and Film E, the similar tendency could be seen that a sharp decrease in the Curie temperature whereas a slight increase in the curie transition enthalpy. Given that there was a dramatic increment in crystallinity, degree of crystallinity increase influence on the changes of curie transition behavior had been out-performing a lower energy barrier during Curie transition meant to reduce the enthalpy.

B. Dielectric Permittivity and Breakdown Strength

1. Dielectric Permittivity under Low Electric Field

Dielectric properties of P(VDF-TrFE-CTFE) in the present work was performed replicate for the identical processing methodologies. Previously it is reported that dielectric properties of normal ferroelectric PVDF-based (co)polymers at a low electrical fields varied with different material processing methodologies [17]. Guan [18], [19] compared systematically the dielectric properties of solution-casting films, hot-pressed P(VDF-HPF) films and stretched films thereof, finding that solution-casting pristine films showed relatively lower permittivity (ε') due mostly to the dipole moments of CF_2 in the crystal perpendicular to the external applied electrical field. Moreover, 2D WAXD diffraction files provided evidence that its c-axis of flat-on predominant crystal lamellae were normal to the glass substrate. Hot-pressed P(VDF-HFP) Film exhibited a higher dielectric constant because of random CF_2 dipole orientation in the edge-on predominated crystal plane. Further, the fact, all the stretched ferroelectric P(VDF-HFP) films showing elevated ε' over the pristine membrane, was due to chain conformation transition induced by the mechanical stretch. Briefly, enhanced dielectric properties could be achieved by control of its microstructure and morphology by means of film processing conditions.

By using broadband impedance analyzer, real dielectric constant (ε'), imaginary dielectric constant (ε''), dielectric loss ($Tan\theta$) were plotted. Fig. 3 (A) presented the real permittivity (ε') of each processing samples as a function of frequency. As presented, ε' for as-treated films decreased nonlinear with increase of frequency in any case. Note that polymer dilute solution vaporizing on substrate gave rise to predominant edge-on oriented film with its thickness less than 300 nm because of nano-confinement effects whilst the films composed the main flat-on oriented crystal plane more than 1000 nm [20], [21]. Affiliated to a family of semi-crystal polymer, bulk-like PVDF-based copolymers and terpolymers formed predominately flat-on oriented crystallites, which had a dipole moment normal to the external electric field due to its

c-axis perpendicular to the substrate. Pristine solution-casting films without post-annealed process had the considerable lower ε' of 26.8 at 0.1 Hz amongst, which might be mostly ascribed to both a CF_2 dipole orientation perpendicular to the electric field in a predominant flat-on crystallite and relatively lower crystallinity fraction. It was observed that SCANL Film B showed much higher ε' than its SCNON pristine Film A, approximately 40.6 at 0.1 Hz. For intermediate crystallized solution casting film, dipole moments of the CF_2 and the fluorinated repeated units defects (CTFE) distributed perpendicular to the external field inhomogeneously because of existence of comparatively rigid spatial hindrance in the polymer chain within crystal region. Therefore, the dipole moments did not align with or were not capable of being parallel with the external electric field to large extent. For post-annealed samples presented in Fig. 3 (A), the molecular chain moved simultaneously and reached thermal and dynamic equilibrium intrinsically when annealing at a given temperature close to the melting point, leading to an elevated crystallinity fraction. In this case, more dipoles parallel to the electric field were induced, resulting in the large orientation polarizability. In order to elucidate crystal orientation effects, fully crystalized film B was stretched in a large tensile ratio of 700% aiming to obtain edge-on crystal lamellae films. Intriguingly, SC-Stretched Film C showed the largest ε' among the casted film sets although slight crystallinity fraction loss was observed. Reportedly, the molecular chain c-axis of the crystals were aligned along the stretching direction because molecular tie could transfer the force loading effectively. The crystal lamellae slipped between each neighboring crystal lamellae and consequently, c-axis of crystal lamellae were consistent with stretching force. A quantitative CF_2 dipole would align with the electric field, resulting in an out-performed dielectric constant. Such results suggested that the coexistence of varying crystal lamellae orientation in the casted films.

As hot-pressed Film E in slowly cooling rate, the highest real permittivity was observed due to the predominated edge-on crystal lamellae induced by force compression of terpolymer in molten state. Interestingly, hot-pressed had a lower crystallinity over stretched SC Film C but a higher dielectric constant. That means large amount of dipoles moment alignment with applied external electric field over stretched film C. The fact was probably due to larger amount edge-on crystal lamellae induced by hot-pressing process.

Dielectric relaxation properties of P(VDF-TrFE-CTFE) processing condition dependent were also investigated by imaginary parts of dielectric spectra ε'' and dielectric loss $Tan\theta$ as shown in Fig. 3 (B). Each samples studied showed two relaxation peaks both at low electric field frequency (less than 1 Hz) and at high frequency field (~ 1 MHz). The relaxation peak at low frequencies originated from the three combined effects of relaxation: Maxwell-Wagner-Sillars (MWS) relaxation, electrode polarization and DC conductivity. Given that electrode polarization (atomic polarization was suppressed and quite low intensity magnitude order), amorphous dipole segmental relaxation, charge carrier ion

motion or conductivity attributed to the lower frequency at room temperature. At low electric field frequency, SCNON pristine Film A exhibited considerably larger dielectric relaxation peaks over isothermal crystallized Film B and stretched Film C, which showed lowest peak amplitude amongst. It is supposed [22], [23] that dielectric relaxation at low frequency referred to DC conductivity contributing factor at higher temperature above ambient temperature. In this case, relaxation regimes in a relative low frequency were overlapped by conductivity process as presented in Fig. 3 (B). In higher frequency large relaxation process was associated with segmental chain motion and thus this typical relaxation type- α originated from the long-term molecular chain sequence motions aligned with the dipole moments of inter-chains switching in amorphous phase upon the external electric field. Pronouncedly, one could readily conclude that processing methodologies played a crucial role to the molecular chain mobility for terpolymer films. It was worth noticing that hot-pressed quenching film D had rather low relaxation peak in lower frequency whilst rather high relaxation were observed for its homological hot-pressed cooling films. Both MWS effect and conductivity factor could rationalize the phenomena and the contributing factor would be analyzed later. Additionally, in high frequency as-casted stretched Film C saw an intense α-relaxation peak. However, its peaks position shifted toward low frequency suggesting a slowing down of relaxation rate and enhanced relaxation time. More constrained interface molecules attaching to crystal lamellae as contributing factor rationalized the sum of dielectric relaxation parts. Thus, constrained molecular mobility was induced by mechanical stretch process. On the other hand, hot-pressed quenching film showed quite similar structure relaxation spectra in high frequency as non-annealed pristine film A. No discernible evidence showed somewhat shift of peak position of hot-pressed cooling Film E besides an enhanced intensity of relaxation peak.

2. Breakdown Strength of Films

High dielectric constant materials in combination with high breakdown electric strength were desired in large-scale application fields as electric vehicles, medical devices and high energy weapon system. It was reported that high dielectric constant P(VDF-TrFE) with quite high energy storage density, due to high electric breakdown strength by tuning its dipole moment before reaching the polar displacement saturation, were developed and found as a good candidate for electronic layer dielectrics. In an attempt to obtain out-performed electrostrictive response, high electric field must be applied to ferroelectric unimorphs. Xu [24] reported that irradiated P(VDF-TrFE) copolymer performed rather high permittivity and electrostrictive response. Its relaxation peak position shifted depending on the frequency over isothermal dielectric spectra. This implied a relaxor ferroelectric behavior. Inspired by this case, CTFE acted as defects were introduced into copolymer backbone, disturbing the molecular chain conformation. Larger interfacial polarization was seen and resulted in elevated electric

breakdown strength. In parallel, many have been considered to enhance this desirable property. Physical or chemical processing methods were conducted to the PVDF-based copolymer/terpolymers films, generating high dielectric permittivity films concomitant with electric breakdown strength. By control of morphology and microstructure of crystallites, films with high constant permittivity and energy storage density were achieved. Recently, study was dedicated to enhance the electric breakdown strength through cross-linked polymer networks photo- and thermally-induced methods. Resultant polymer films possessed greatly enhanced energy storage density on expense of mechanical behavior losses unfortunately.
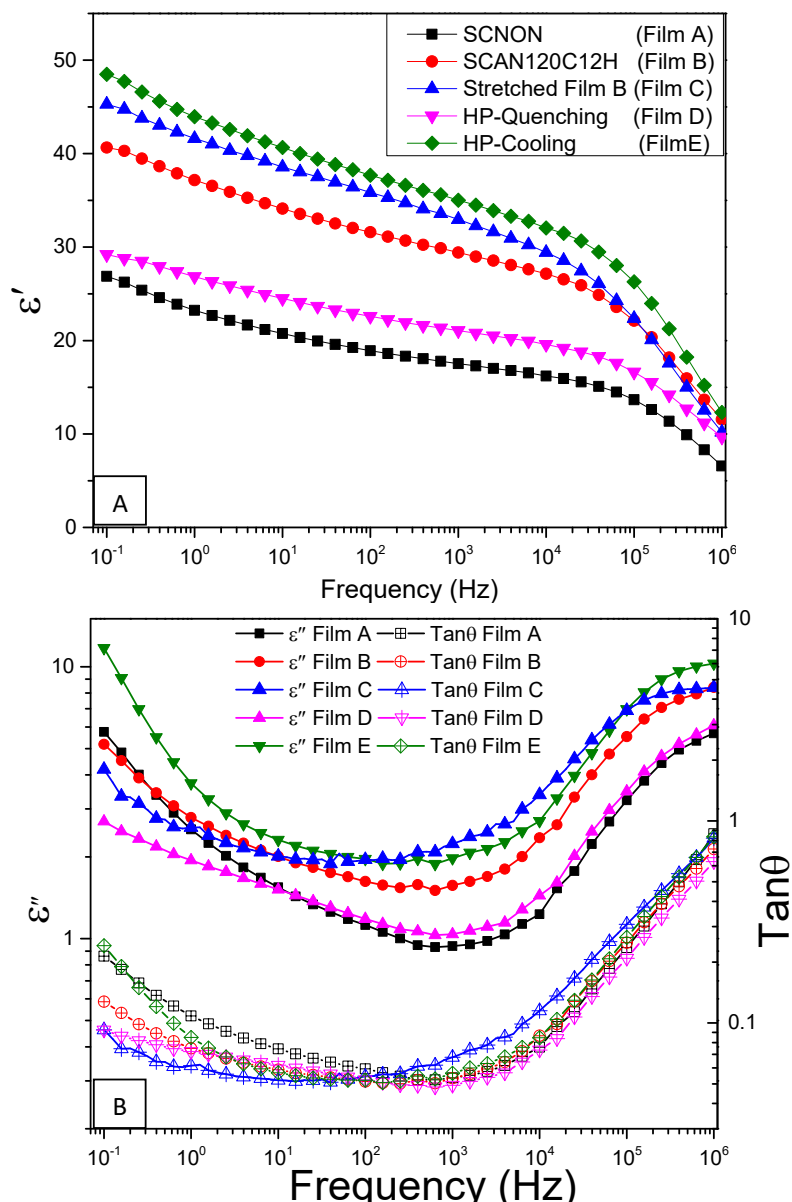

Fig. 3 Dielectric permittivity extrapolated from isothermal dynamic dielectric spectroscopy at room temperature 25℃; (A) dielectric constant over a full large scale of frequency for as-prepared terpolymer films, lines are guide by eyes; (B) dielectric loss spectra and loss tangent θ

As stated, breakdown strength was microstructure and chemical composition dependent, which were mainly associated with processing condition. In this current work, at least 20 replicate manipulations were carried out to fulfill the Weibull breakdown statistics. And breakdown strength E, breakdown probability ($P(E)$) were calculated by two parameters Weibull exponential equation, $P(E) = 1 - \exp[-(E/\lambda)^k]$, where λ is the scale parameter reflecting the breakdown electric strength where 63.2% probability of the breakdown occurred; k is the shape parameter of distribution

spread. As presented in Fig. 4, Weibull probability fitting to each as-casted and hot-pressed films were plotted. It was observed that electric breakdown strength value for as-casted pristine Film A at 223.9 MV/m was much lower than fully-crystalized film B at 340.4Mv/m, the highest value amongst. Intriguingly, hot-pressed quenching films showed slight lower breakdown strength over the pristine Film A. Nonetheless, small augmentation was observed when concerning the electric breakdown values of hot-pressed cooling films. For non-linear dielectric fluorinated polymers, thin films showed a peak mode in its relative permittivity, with the decrease at high and low electric field. The measured values implied that E_b was significantly dependent upon degree of crystallinity for as-casted terpolymer films. Electric resistivity between polymer chains was much larger than along them. Thus crystal lamellae composed by well-ranged molecular chain folds appeared to lead to a higher breakdown strength value due to reduced amorphous phase content where molecular chain

entangled disorderedly. In contrary, terpolymer films possessing more amorphous phase showed less electric resistivity, resulting in the lower breakdown strength values. Besides, because of large interfacial polarization, one should not neglect the interface scattering effects to the piled charges carrier ions. Elevated crystal lamellae density in favor of more interactions involved in the interfacial area where the charge carrier ions aggregations evenly distributed. This could lead to the higher resistivity and higher breakdown strength. Hot-pressed film D exhibited lower electric breakdown values than as-casted films although the both shared the identical degree of crystallinity. Impurity must contribute to this increase gap. Raw polymer powder would be purified by means of casting during which non soluble residual precipitated. This could lead to polymer solution with reduced impurity. Presence of impurity causes the raise of electric breakdown probability significantly, resulting in a decrease of breakdown strength values.
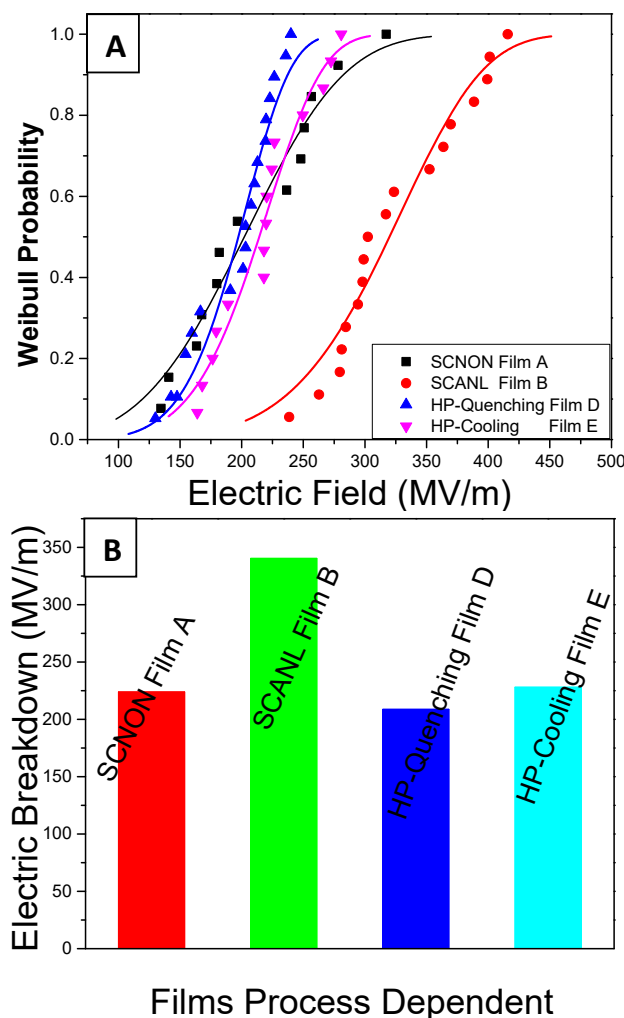

Fig. 4 (A) Weibull distribution (Probability) in a high electric field breakdown strength for at-treated thin films; (B) Breakdown strength of as-casted pristine Film A and fully-crystalized film in comparison with hot-pressed quenching Film D and cooling Film E

C. Electromechanical Properties

1. Mechanical Behaviors

Young's modulus, one of crucial mechanical properties of electromechanical candidate films was relevant to its crystal microstructure and morphology controlled by processing condition. Established literatures reported that enhanced thermal and mechanical resistance were observed for the most known engineering polymer, PS, PE, PET , PVc , PP, etc in concomitant with increase of overall crystallinity fraction.
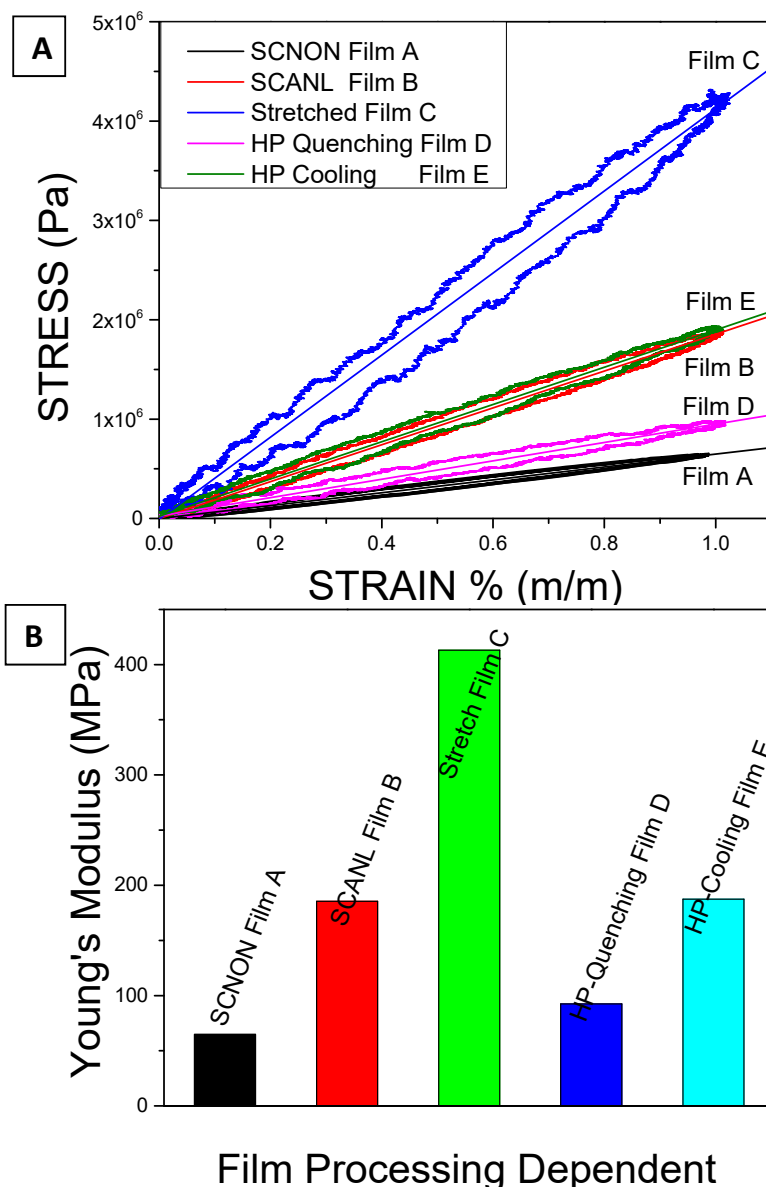

Fig. 5 (A) Strain-stress curves in a sinusoidal functional mode for as-treated terpolymer films (B) Young's Modulus comparison dependent upon polymer processing for as-casted, stretched and as hot-pressed methods

Interestingly, it could be observed that an incremental of Young's modulus correlated with processing in Fig. 5. A strongly enhanced Young's modulus was noted from 64.9 MPa for as casted pristine Film A to third folds increase in 185.5MPa for fully isothermally crystalized terpolymer film B, while only 6% crystallinity augmentation witnessed in Table I, showing that Young's modulus was extremely sensitive to the degree of crystallinity. It was worth noticing that stretched terpolymer C had much higher Young's modulus at 413.0 MPa in the fully around 700% fully-stretched state. As presented in Fig. 2, initially entangled molecular chain in amorphous phase were stretched to somewhat extent and its orientation crystal lamellae, acting as fixed phase, aligned with stretching direction. Moreover, inter-crystal lamellae

connecting molecules tie prevent the progress of molecular slip or deformation [25]. On the other hand, hot pressed quenching films had slight higher Young's modulus than as-casted pristine Film A which could be ascribed to little more degree of crystallinity fraction. However, hot-pressed cooling films possessed equivalent modulus values as isothermal annealed Film B which suggested hot-pressing and as-casting process showed no significant disparity for Young's modulus.

2. Electrostrictive Behaviors

Besides high breakdown strength behavior associated with processing condition, Young's modulus could determine the electromechanical behavior to somewhat extent as an instrumental parameter. Electromechanical response was evaluated by electrostrictive properties. In this current work, polymer samples with normalized dimension were subjected to the 0.1Hz altering current high electric field in a cantilever beam mode. In molecular level, the external electric filed induced a reversible molecular conformation change from mixture of TG^+TG^- and $T_3G^+T_3G^-$ (less-ordered ferroelectric phase) to the all-*Trans* chain conformation, resulting in the electrostrictive deformation apparently. Thus this electroactive polymer showed rather high mechanical elastic energy density according to $YS_{M31}^2/2$ equation where Y denotes young's modulus of processed active polymer and S_{M31} is transverse stain of a cantilever beam. This made it as a rather good candidate for sensor and actuator implementation.

The apparent transverse strain response curves along the length direction, normal to the films and applied electric field were plotted against the varying electric field for each as-casted, stretched and hot-pressed processed films as shown in Fig. 6. It was observed that each transverse strain curve were nonlinear and highly dependent upon the electric field. Noticeably, transverse strain at given electric filed for each processed films varied and well fitted to quadratic function, suggesting apparent electrostrictive deformation were quadratic relationship with applied electric field. And fitting record and related parameters were summarized in Table II. Intriguingly, transverse strain was inversely proportional to degree of crystallinity and Young's modulus for each as-treated films at given electric field of 20 MV/m. Pristine Film A presented the largest strain amongst, further more than 4 times higher over the fully crystallized Film B which only had 0.0528% out-of-plane strain. Eury reported that electrostrictive coefficient correlated with reciprocal of $\varepsilon_0\varepsilon'_rY$. Young's modulus value of fully-crystallized film was 3 times higher than that of pristine Film A but with its dielectric permittivity only no more than twice higher. Exceptionally, stretched Film C behaved 0.0754% transverse strain since the young's modulus was twice over the original Film B. Hot-pressed quenching film had the largest transverse strain rather a slight higher dielectric permittivity. Its dielectric and interfacial polarization were equivalent to the pristine Film A quantitatively. However, dielectric loss in Film D was much lower than losses in pristine Film A, therefore, multiplied electric energy was transferred to the mechanical elastic energy by which large transverse strain were rationalized.

Moreover, much lower transverse strain was obtained for hot-pressed Film E. Such results must be due to the large dielectric loss in low electric frequency and relatively high Young's modulus also showed negative effects.
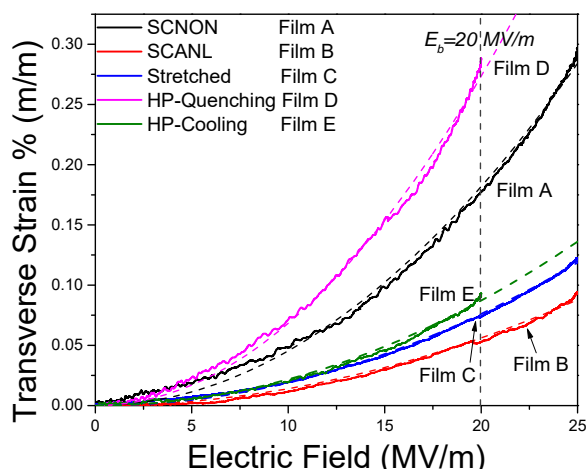

Fig. 6 Transverse stain curves versus electric field for as-casted isothermal crystallized and hot-pressed terpolymers films

In an attempt to fully picture the relation between polymer microstructure and electromechanical energy density chemically and physically, transverse elastic energy density $YS_{M31}^2/2$ were calculated. Due to its largest transverse strain, mechanical energy density $YS_{M31}^2/2$, pristine Film A possessed the rather high value up to 102.1 J/m^3 amongst. In contrary, the desired high degree of crystallinity and large dielectric constant afforded the lowest elastic energy density as 25.45 J/m^3 instead. Hot-press polymer tended to afford the polymer film with high mechanical elastic energy density. Especially for Hot-press quenching films, 359.5 J/m^3, the highest energy density value was observed instead HP-Cooling film possessed one fifth fraction. Such results implied electromechanical behaviors were significantly dependent upon the film processing condition.

IV. CONCLUSION

In this present study, electroactive relaxor ferroelectric P(VDF-TrFE-CTFE) films were fabricated by varying film thermal and mechanical stretching or hot-press processing methodologies. And mechanical elastic energy density was evaluated by the cantilever beam mode experimental setup. It was found that degree of crystallinity could be elevated by isothermal crystallization at high temperature, resulting in the enhancement of dielectric and mechanical Young's modulus properties. By stretching process, annealed films give rise to high dielectric constant and mechanical behavior. This could afford an exceptional increase of mechanical elastic energy density. In addition, films by hot-press process exhibited rather high electrostrictive response and also surprisingly high values of E_μ in hot-press quenching films. On basis of as-mentioned results, E_μ for P(VDF-TrFE-CTFE) films were highly processing correlated. These features allow the

processed active relaxor ferroelectrics utilized in sensor and actuator, especially microelectromechanical systems.

TABLE II

DATA COLLECTIONS OF TRANSVERSE STRAIN (S_{31}), YOUNG'S MODULUS (Y), MECHANICAL ENERGY DENSITY (E_μ), FITTED APPARENT ELECTROSTRICTIVE COEFFICIENT (M) PROCESSING DEPENDENT

Processed Polymers	χ_C %	S_{31}[%] at 20 MV/m	Y (MPa)	${}^{a}E_\mu$ (J/m^3)	${}^{b}M_{31}\cdot E\text{-}18$ $(m^2/V^2)^b$	ε'_r (0.1 Hz)
Film A SC NON	12.63	0.1774	64.9	102.1	4.55	26.87
Film B 120C12H	18.56	0.0528	182.5	25.45	1.40	40.65
Film C Stretched	17.13	0.0754	413.0	117.4	1.90	45.28
Film D HP-Quenching	14.29	0.2788	92.5	359.5	6.84	29.30
Film E HP-Cooling	16.74	0.0887	182.7	71.87	2.18	48.50

Note: a, E_μ, maximum elastic electric energy density could be simplified as $YS_{M31}{}^2/2$, vacuum permittivity, $\varepsilon_0 = 8.854187 \times 10^{-12}$ F/m; b, apparent electrostictive coefficient extrapolated from quadratic fitting curve.

REFERENCES

[1] Park, C., et al., *Actuating single wall carbon nanotube-polymer composites: intrinsic unimorphs.* Advanced Materials, 2008. 20(11): p. 2074.

[2] Carpi, F., et al., *Dielectric elastomers as electromechanical transducers: Fundamentals, materials, devices, models and applications of an emerging electroactive polymer technology.* 2011: Elsevier.

[3] Zhao, X.L., et al., *Enhanced dielectric and ferroelectric properties in the artificial polymer multilayers.* Applied Physics Letters, 2014. 104(8): p. 082903.

[4] Haines, C.S., et al., *Artificial muscles from fishing line and sewing thread.* science, 2014. 343(6173): p. 868-872.

[5] Huang, M., et al., *Nanomechanical architecture of semiconductor nanomembranes.* Nanoscale, 2011. 3(1): p. 96-120.

[6] Zhang, Q., V. Bharti, and X. Zhao, *Giant electrostriction and relaxor ferroelectric behavior in electron-irradiated poly (vinylidene fluoride-trifluoroethylene) copolymer.* Science, 1998. 280(5372): p. 2101-2104.

[7] Chu, B., et al., *A dielectric polymer with high electric energy density and fast discharge speed.* Science, 2006. 313(5785): p. 334-336.

[8] Buckley, G., et al., *Electrostrictive Properties of Poly (vinylidenefluoride-trifluoroethylene-chlorotrifluoroethylene).* Chemistry of Materials, 2002. 14(6): p. 2590-2593.

[9] Bao, H.M., et al., *Phase transitions and ferroelectric relaxor behavior in P(VDF-TrFE-CFE) terpolymers.* Macromolecules, 2007. 40(7): p. 2371-2379.

[10] Cheng, Z.-Y., et al., *Electrostrictive poly (vinylidene fluoride-trifluoroethylene) copolymers.* Sensors and Actuators A: Physical, 2001. 90(1): p. 138-147.

[11] Kremer, F., *Broadband dielectric spectroscopy.* 2003: Springer Science & Business Media.

[12] Garrett, J., et al., *Electrostrictive behavior of poly (vinylidene fluoride-trifluoroethylene-chlorotrifluoroethylene).* Applied Physics Letters, 2003. 83(6): p. 1190-1192.

[13] Neese, B., et al., *Large electrocaloric effect in ferroelectric polymers near room temperature.* Science, 2008. 321(5890): p. 821-823.

[14] Smith, O.N.L., et al., *Enhanced Permittivity and Energy Density in Neat Poly (vinylidene fluoride-trifluoroethylene-chlorotrifluoroethylene) Terpolymer Films through Control of Morphology.* ACS applied materials & interfaces, 2014. 6(12): p. 9584-9589.

[15] Tan, S., et al., *Significantly improving dielectric and energy storage properties via uniaxially stretching crosslinked P (VDF-co-TrFE) films.* Journal of Materials Chemistry A, 2013. 1(35): p. 10353-10361.

[16] Yang, L., et al., *Relaxor Ferroelectric Behavior from Strong Physical Pinning in a Poly(vinylidene fluoride-co-trifluoroethylene-co-chlorotrifluoroethylene) Random Terpolymer.* Macromolecules, 2014. 47(22): p. 8119-8125.

[17] Gregorio Jr, R. and E. Ueno, *Effect of crystalline phase, orientation and temperature on the dielectric properties of poly (vinylidene fluoride)(PVDF).* Journal of Materials Science, 1999. 34(18): p. 4489-4500.

[18] Guan, F., et al., *Crystal orientation effect on electric energy storage in poly (vinylidene fluoride-co-hexafluoropropylene) copolymers.* Macromolecules, 2009. 43(1): p. 384-392.

[19] Guan, F., et al., *Effects of polymorphism and crystallite size on dipole reorientation in poly (vinylidene fluoride) and its random copolymers.* Macromolecules, 2010. 43(16): p. 6739-6748.

[20] Wang, J., et al., *Transition from relaxor to ferroelectric-like phase in poly (vinylideneflouride-trifluoroethylene-chloroflouroethylene) terpolymer ultrathin films.* Applied Physics Letters, 2011. 98(5): p. 052906.

[21] Li, Q., et al., *Solution-processed ferroelectric terpolymer nanocomposites with high breakdown strength and energy density utilizing boron nitride nanosheets.* Energy & Environmental Science, 2015. 8(3): p. 922-931.

[22] Furukawa, T. and T. Wang, *Measurements and properties of ferroelectric polymers.* Vol. 5. 1988: Chapman and Hall: New York.

[23] Hahn, B., J. Wendorff, and D.Y. Yoon, *Dielectric relaxation of the crystal-amorphous interphase in poly (vinylidene fluoride) and its blends with poly (methyl methacrylate).* Macromolecules, 1985. 18(4): p. 718-721.

[24] Xu, H., et al., *Ferroelectric and electromechanical properties of poly (vinylidene-fluoride–trifluoroethylene–chlorotrifluoroethylene) terpolymer.* Applied Physics Letters, 2001. 78(16): p. 2360-2362.

[25] You, J., et al., *Crystal Orientation Behavior and Shape-Memory Performance of Poly (vinylidene fluoride)/Acrylic Copolymer Blends.* The Journal of Physical Chemistry B, 2012. 116(4): p. 1256-1264.